Cazenave, Marine and Radovčić, Davorka (2023) *The Neanderthal patellae from Krapina (Croatia): A comparative investigation of their endostructural conformation and distinctive features compared to the extant human condition.* American Journal of Biological Anthropology, 181 (1). pp. 118-129. ISSN 2692-7691.

BRIEF COMMUNICATION

AMERICAN JOURNAL OF
BIOLOGICAL ANTHROPOLOGY
The Official Journal of the American Association of Biological Anthropologists

WILEY

The Neanderthal patellae from Krapina (Croatia): A comparative investigation of their endostructural conformation and distinctive features compared to the extant human condition

Marine Cazenave [1,2,3] 🔾 | Davorka Radovčić [4]

[1] Division of Anthropology, American Museum of Natural History, New York, New York, USA

[2] Skeletal Biology Research Centre, School of Anthropology and Conservation, University of Kent, Canterbury, UK

[3] Department of Anatomy, Faculty of Health Sciences, University of Pretoria, Pretoria, South Africa

[4] Department of Geology and Paleontology, Croatian Natural History Museum, Zagreb, Croatia

Correspondence
Marine Cazenave, Division of Anthropology, American Museum of Natural History, New York, NY, USA.
Email: marine.cazenave4@gmail.com

Funding information
American Museum of Natural History

Abstract

Objectives: The Neanderthal patella differs from that of extant humans by being thicker anteroposteriorly and by having more symmetric medial and lateral articular facets. However, it is still unclear to what extent these differences affect knee kinesiology. We aim at assessing the endostructural conformation of Neanderthal patellae to reveal functionally related mechanical information comparatively to the extant human condition. In principle, we expect that the Neanderthal patella (i) shows a higher amount of cortical bone and (ii) a trabecular network organization distinct from the extant human condition.

Materials and Methods: By using micro-focus X-ray tomography, we characterized the endostructure of six adult patellae from the OIS 5e Neanderthal site of Krapina, Croatia, the largest assemblage of human fossil patellae assessed so far, and compared their pattern to the configuration displayed by a sample of 22 recent humans.

Results and Discussion: The first expectation is rejected, indicating that the patellar bone might have not followed the trend of generalized gracilization of the human postcranial skeleton occurred through the Upper Pleistocene. The second prediction is at least partially supported. In Krapina the trabecular network differs from the comparative sample by showing a higher medial density and by lacking a proximal reinforcement. Such conformation indicates similar load patterns exerted in Neanderthals and extant humans by the vastus lateralis, but not by the vastus medialis, with implications on the mediolateral stabilization of the knee joint. However, the patterns of structural variation of the patellar network remain to be assessed in other Neanderthal samples.

KEYWORDS
internal structure, Neanderthal, patella

1 | INTRODUCTION

In European and Near Eastern Neanderthals, the morphology of the patella differs from the typical condition of extant humans (EHs) by being absolutely and relatively thicker anteroposteriorly and by having more symmetric medial and lateral articular facets associated with a more centrally positioned articular ridge and higher angles between the medial and lateral margins of the articular facets and the ridge (e.g., Boule, 1911–1913; Heim, 1982; Rosas et al., 2020; Trinkaus, 1983a, 2000; Trinkaus & Rhoads, 1999; Trinkaus et al., 2017; Vandermeersch, 1981). A recent geometric morphometric analysis of the assemblage from El Sidrón, Spain, has shown that the typically thick Neanderthal patella with symmetrical contact surfaces tends to be accompanied by a distally positioned lateral mass compared to the more central position observed in EH (Rosas et al., 2020). Conversely, overlapping proportions between the two taxa have been recorded for the kneecap maximum height and breadth (Rosas et al., 2020). In Neanderthals, along with a posterior displacement relative to the diaphyseal axes of the tibial tuberosity and condyles of the knee joint capsule and of the ligament attachments (e.g., Boule, 1911–1913; Fraipont, 1888; Heim, 1982; Lustig, 1915; Trinkaus, 1983a; Vandermeersch, 1981), a thicker patella has been suggested to increase the quadriceps femoris moment arm in the knee joint, thus making the Neanderthal legs more powerful in extension (Chapman et al., 2010; Miller & Gross, 1998; Trinkaus, 1983b). However, a close relationship between the degree of patellar facet asymmetry and the configuration of the distal femur has been questioned (Trinkaus & Rhoads, 1999). Indeed, while a more expanded lateral facet of the EH patella has been related to the medial tibiofemoral angle (Hartigan et al., 2011; Rosas et al., 2020), bicondylar angles in Neanderthal femora associated to more symmetric patellar facets are not distinguishable from those measured in EH (Tardieu & Trinkaus, 1994; Trinkaus, 2006). Accordingly, it does not appear to be a tight relationship between degree of patellar facet asymmetry and articular configuration of the distal femur and it is still unclear to what extent variation in patellar articular proportions affects knee kinesiology (Trinkaus, 2000).

More recently, it has been proposed that, compared with the *Homo sapiens* derived morphology, the condition of the Neanderthal patellar articular surfaces is related to a rotation of the tibia with respect to the distal femur, implying a mediolateral displacement of the patellar ligament which would increase contact force of the patella with the femoral condyles and affect the functional space for the expansion of the facets (Rosas et al., 2020).

Given the ability of the mechanosensitive cortical and trabecular bony tissues to adjust structurally during life to the site-specific loading environment (e.g., Hoechel et al., 2015; Katoh et al., 1996; Mazurier, 2006; Mazurier et al., 2010; Raux et al., 1975; Toumi et al., 2006, 2012; Townsend et al., 1975; Van Kampen & Huiskes, 1990), the assessment of patellar endostructural features such as cortical bone thickness variation and trabecular network arrangement have the potential to provide subtle functionally related information about the knee joint mechanical environment (Cazenave

et al., 2019; Cazenave et al., 2022). A preliminary comparative study noninvasively investigating the inner organizational pattern of the adult patella in two Neanderthals (from Krapina, Croatia, and Regourdou, France), one anatomically modern fossil human (the Magdalenian from Chancelade, France), and in a sample of African- and European-derived Holocene individuals revealed marked differences not only between the Neanderthal and the fossil and Holocene humans, but also between the two Neanderthal specimens (Cazenave et al., 2020). Interestingly, despite a general reduction trend in postcranial skeletal robusticity recorded from the Upper Pleistocene through the Holocene (Chirchir et al., 2015, 2017; Ruff et al., 2015; Ryan & Shaw, 2015; Scherf et al., 2016), the analyses did not reveal any tendency toward gracilization for all quantitative parameters reflecting bone robusticity considered in the study (Cazenave et al., 2020). Nonetheless, this evidence needs confirmation from a larger sample. Additionally, the existence of a set of distinctive inner features uniquely characterizing the Neanderthal patella needs to be verified and the extent of the differences in endostructural conformation (patterns) between Neanderthals and EH remains to be assessed.

Here we apply 2D and 3D techniques of virtual imaging to an X-ray microtomographic record to quantitatively characterize the internal structure of six patellae from the Neanderthal site of Krapina, Croatia, and compare the results to the EH condition (Cazenave et al., 2019, 2020; Hoechel et al., 2015; Toumi et al., 2006, 2012). In principle, we expect that the Neanderthal assemblage (i) shows, on average, a higher amount of cortical bone than measured in the comparative human sample used in this study and, based on the outer characteristics distinguishing the Neanderthal from the modern human patella (Rosas et al., 2020; Trinkaus, 2000). We also expect that the fossil patellae (ii) possess some features in both cortical bone topographic distribution and site-specific organization of the trabecular network clearly distinct from the EH condition, thus allowing to identify a unique Neanderthal endostructural pattern.

2 | MATERIALS AND METHODS

2.1 | Materials

The fossil sample consists of three right and three left patellae representing a minimum of four (see below) Neanderthal adult individuals of unknown sex selected because of their relative preservation conditions from the assemblage of 16 patellae from the Eemian (OIS 5e) Croatian site of Krapina (Kricun et al., 1999; Radovčić et al., 1988; Rink et al., 1995).

The specimen Krapina 215.1-Pa. 1 (hereafter referred as Pa. 1) is a right patella with minimal erosion along the proximal, distal and lateral margins and the distal part of the medial facet (Figure 1a). Based on comparative size and morphology, Pa. 1 could belong to the same individual represented by the specimen 216.1-Pa. 5 (Trinkaus, 1975, 2000). Krapina 215.3-Pa. 3 (Pa. 3) is also a right patella with minimal damages in the distal margin of its posterior aspect (Figure 1b). Originally suggested to represent the same individual of 215.2-Pa. 2 (Trinkaus, 1975),
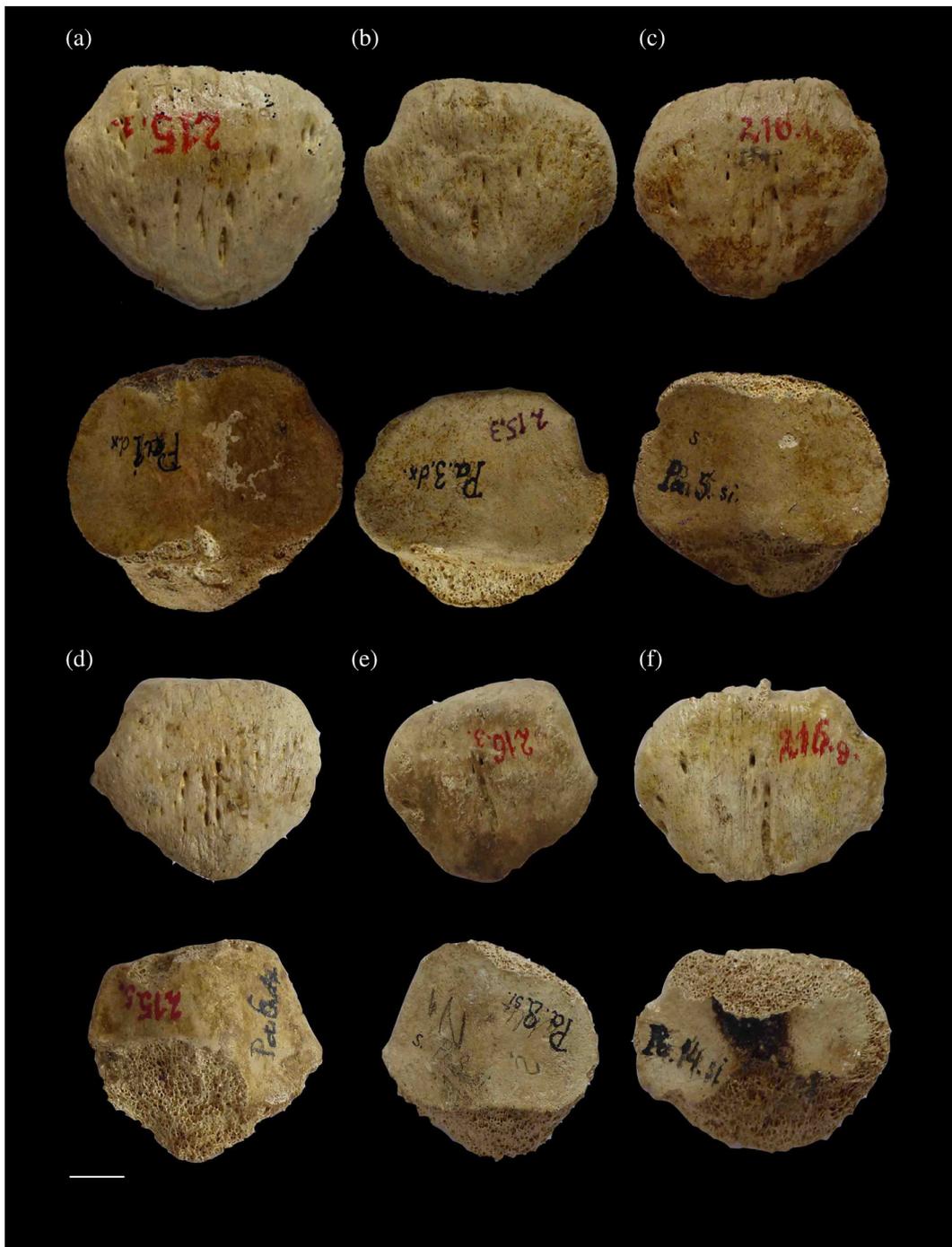
FIGURE 1 Anterior (upper row) and posterior (lower) views of the right patella 215.1-Pa. 1 (a), the right patella 215.3-Pa. 3 (b), the left patella 216.1-Pa. 5 (c), the right patella 215.5-Pa. 6 (d), the left patella 216.3-Pa. 8 (e), and the left patella 216.9-Pa. 14 (f) forming the Neanderthal sample from Krapina, Croatia, considered in this study. All specimens are from adult individuals. Scale bar: 1 cm.

not included in this study, Pa. 3 has been later tentatively associated to the specimen 216.9-Pa. 14 (see above; Trinkaus, 2000). The fossil 216.1-Pa. 5 (Pa. 5), which could represent the same individual of Pa. 1 (Trinkaus, 1975, 2000) and which has been previously reported for its general inner conformation (Cazenave et al., 2019), is a left patella with some erosion along the proximal, lateral and medial articular margins and the posterior aspect of the apex (Figure 1c). Krapina 215.5-Pa. 6 (Pa. 6) is a right patella bearing some damages on the proximal and distal portions of the medial articular surface (Figure 1d). The specimen 216.3-Pa. 8 (Pa. 8) is a left patella displaying minor abrasion on the proximal, medial and distal edges (Figure 1e). Finally, the left patella 216.9-Pa. 14 (Pa. 14), perhaps associated to Pa. 3, is the least preserved specimen within the fossil assemblage considered here (Figure 1f). Its mediolateral and anteroposterior diameters are preserved, but it lacks the proximal third of the articular surface and the distal extremity of the apex.

4 WILEY AMERICAN JOURNAL OF BIOLOGICAL ANTHROPOLOGY
The Official Journal of the American Association of Biological Anthropologists

CAZENAVE and RADOVČIĆ

It also shows erosion and damages on the distal third of the posterior aspect.

Descriptive and quantitative information on this fossil assemblage, including height, width, thickness, and metrics of the medial articular and lateral facets, can be found in Gorjanović-Kramberger (1906), Trinkaus (1975, 2000), Radovčić et al. (1988), Rosas et al. (2020) (for Pa. 5, see also Cazenave et al., 2019). Ten of the 16 patellae forming the entire Krapina assemblage, including five of six among those considered in this study, have been previously imaged in the radiographic atlas of the Krapina's human remains (Kricun et al., 1999; figure 123). All fossils are housed at the Croatian Natural History Museum, Zagreb.

The EH comparative material consists of 22 finely preserved adult patellae from individuals of both sexes, all from the right side and lacking macroscopic evidence of alteration or pathological changes. The assemblage represents eight individuals of African ancestry (four males and four females aged 22–32 years) and seven of European ancestry (three males and four females aged 21–51 years) selected from the Pretoria Bone Collection stored at the Department of Anatomy of the University of Pretoria, South Africa (L'Abbé et al., 2005), and seven patellae (from two likely male and five likely female individuals whose estimated age at death ranges between c. 30 and c. 50 years) from the Imperial Roman graveyard of Velia, Italy, stored at the "Luigi Pigorini" National Museum of Prehistory and Ethnography (rev. in Beauchesne & Agarwal, 2017).

To test the possible influence of laterality, we also used an additional set of left patellae (representing three males and five females of both African and European ancestry) belonging to eight among the 15 individuals forming the comparative sample from the Pretoria Bone Collection. This additional set was uniquely used for testing laterality. Details on the composition of the EH sample are provided as Table S1.

2.2 | Methods

The patellae from Krapina were imaged by X-ray microtomography (μXCT) at the Multidisciplinary Laboratory of the International Centre for Theoretical Physics (ICTP) of Trieste, Italy (Tuniz et al., 2013), at an isotropic voxel dimensions of 33 μm. The archeological specimens from Velia were also imaged at the ICTP at an isotropic voxel size ranging from 25 to 29 μm. The specimens from the Pretoria Bone Collection were scanned at the South African Nuclear Energy Corporation (Necsa), Pelindaba, with an isotropic voxel size ranging from 24 to 59 μm (Table S1). Following acquisitions, a virtual transformation of each dataset has been carried out to coherently orient all specimens by using Avizo v.8.0.0. (Visualization Sciences Group Inc.). More specifically, each image stack has been manually rotated, until the most lateral and medial surface junctions between the apex and articular surface in posterior view are aligned with the x-axis, the most lateral and medial points in proximal view are aligned with the y-axis, and the articular surface in medial view is aligned with the z axis. The new image stack orientation has then be saved in Avizo by resampling the data.

In each specimen, we firstly delimited the cortico-trabecular complex (CTC), that is, the component which includes the cortical shell (lamina) and the intimately related adjoining portions of the supporting denser trabecular network (Cazenave et al., 2019, 2020; Mazurier, 2006; Mazurier et al., 2010). By using the routine MPSAKv2.9 (in Dean & Wood, 2003), we measured the CTC mean thickness (CTT) across the anterior (aCTT) and posterior (pCTT) surfaces by using the sagittal and the transversal slices respectively extracted at the maximum anteroposterior thickness and the mediolateral breadth (Figure 2a). Because of damages on their posterior aspects, it was not possible to measure the pCTT across both sagittal and transversal virtual sections in Pa. 6 (Figure 1d), while in Pa. 14 the pCTT was not measured across the sagittal slice (Figure 1f). To conduct size-independent
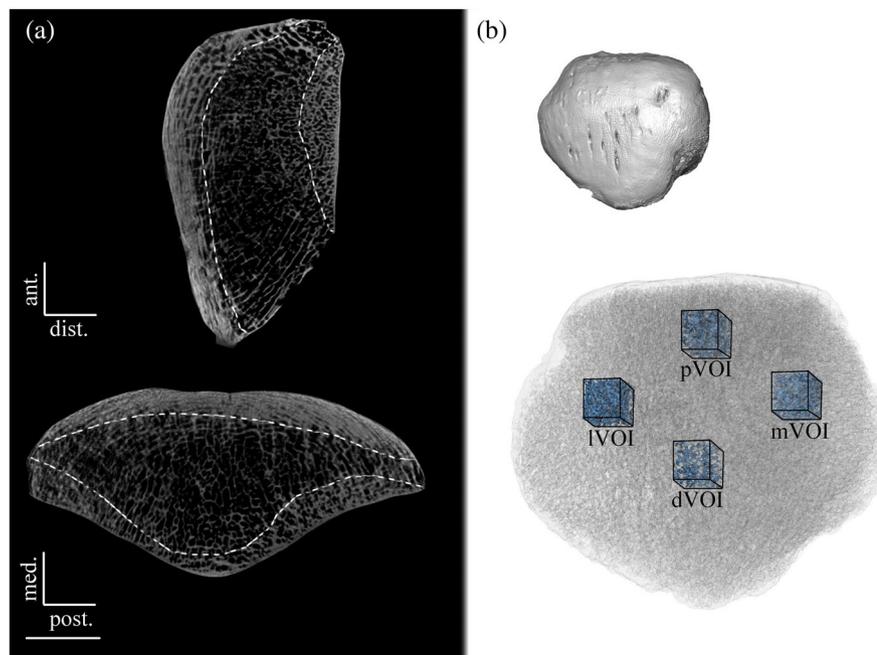
FIGURE 2 Transversal (upper row) and sagittal (lower) virtual sections respectively extracted at the midpoint of the mediolateral breadth and the maximum anteroposterior thickness of Krapina 216.1-Pa. 5 (left patella) showing the limits of the cortico-trabecular complex (CTC) assessed for its average anterior (aCTT) and posterior (pCTT) thickness (a); and microtomographic-based 3D reconstruction of the same specimen (in slightly oblique anterior view) showing the position of the proximal (s), distal (i), medial (m), and lateral (l) cubic volumes of interest (VOIs) extracted for assessing trabecular bone properties. The virtual reconstruction of the outer surface of the specimen (upper, not to scale) is provided for orientation. Scale bar: 1 cm.

CAZENAVE and RADOVČIĆ

AMERICAN JOURNAL OF
BIOLOGICAL ANTHROPOLOGY
The Official Journal of the American Association of Biological Anthropologists

WILEY 5

intra- and inter-taxic comparisons, in each specimen the absolute CTT values (in mm) were standardized with respect to the maximum breadth and provided as percent (%) values in each specimen.

Besides the CTC assessment, in all specimens we also virtually extracted four homologous cubic volumes of interest (VOIs) whose individual edge length systematically equals 10% of the mediolateral maximum patellar breadth. The VOIs systematically sample the proximal (pVOI), distal (dVOI), medial (mVOI), and lateral (lVOI) regions (Figure 2b). The geometric centers of the pVOI and dVOI were placed at the ½ of the mediolateral breadth and of the anteroposterior thickness, and at ¼ of the proximodistal articular height from the proximal and distal margins, respectively. The mVOI and lVOI were positioned at the ½ of the proximodistal articular height and of the anteroposterior thickness, and at ¼ of the mediolateral breadth from the medial and lateral margins, respectively.

To measure the site-specific structural properties of the trabecular network, the cubic VOIs were binarized into bone and air using the "half maximum height" (HMH) quantitative iterative thresholding method (Spoor et al., 1993) and the region of interest protocol (ROI-Tb; Fajardo et al., 2002). Owing to the biasing effects of a nonspherical VOI by using the mean intercept length (MIL) algorithm in Quant3D (Ryan & Ketcham, 2002), on the largest centered sphere fitting completely within each extracted VOI we measured: (i) the trabecular bone volume fraction (BV/TV, in %); (ii) the trabecular thickness (Tb.Th., in mm); and (iii) the degree of anisotropy (DA).

For all variables, a number of intra- and inter-observer tests for accuracy run by independent observers on both the fossil assemblage and on selected specimens from the comparative sample provided differences less or near 4%.

To assess the possible influence of size, in both fossil and comparative extant samples the Pearson's correlation coefficient was calculated between each endostructural variable and the mediolateral breadth of the patella, a dimension found to scale with body size in hominoids (Jungers, 1990; Pina et al., 2014).

Statistical analyses were performed in R v3.4.4 (R Core Team, 2018) by RStudio v1.2.5033, while plots were generated using ggplot2 (Wickham, 2009). Due to small sample sizes, only non-parametric statistical tests were performed. The significance of the differences between the taxa for anterior CTT of the sagittal and transversal sections, BV/TV, Tb.Th. and DA of each VOI was tested by the two-sample t test via Monte-Carlo sampling with 1000 permutations. Given that only four and five fossil specimens could been investigated for the posterior CTT of the sagittal and transversal sections, respectively, we did not conduct, likely unreliable, statistical analyses for this two results. Pairwise Wilcoxon rank sum tests with a Bonferroni correction were used to assess the significance of the intra-taxic differences. A significance threshold of 0.05 for the p values was adopted for all of the statistical analyses.

3 | RESULTS

Besides the cases of the two specimens Pa. 6 and Pa. 14 limitedly to the posterior portion of their CTC, the inner preservation quality of all

fossils from Krapina is suitable for the purposes of a subtle quantitative assessment of their conformation (Figure 3, Supporting Information S1 and Figure S1). As noted in previous studies on the outer morphology of this assemblage (Gorjanović-Kramberger, 1906; Radovčić et al., 1988; Trinkaus, 2000), the anterior aspect of Pa. 3 shows an enthesophyte formation likely resulting from the ossification of fibers of the quadriceps femoris tendon, and the articular surface of Pa. 8 bears minor alterations typical of degenerative changes. However, as previously observed in the case of the Magdalenian patella Chancelade 1 also displaying similar outer degenerative alterations (Cazenave et al., 2019), the μXCT record of both Pa. 3 and Pa. 8 shows that the corresponding underlying cortical and trabecular tissues lack any evident structural change with respect to the surrounding areas, with no evidence of local cortical thinning or thickening and/or trabecular rarefaction or increased density (Figures 3b,e and S1b,e).

3.1 | CTT distribution

In both sagittal and transversal planes, the Neanderthal patellae from Krapina show, on average, a slightly thicker CTT compared to the EH sample used in this study (Table 1, Figure S1) but statistical tests show no significant differences for the anterior CTT of both sagittal and transversal sections. The most marked average differences concern the posterior thickness measured across the sagittal section (7.9% vs. 7.1%) and the anterior thickness across the transversal section (7.3% vs. 6.7%). However, given that the comparative sample shows a wider range of variation for both parameters (4.0%–12.8% and 4.5%–13.1%, respectively, vs. 6.7%–10.6% and 5.9%–9.7% in Krapina), such differences can be considered as negligible. Indeed, even if the Neanderthal patellae show the average thickest cortices (Table S2), for the sagittal and transversal anterior CTT and the transversal posterior CTT the absolute highest values have been measured in humans (Table S2). In terms of cortical thickness topographic distribution, it does not matter the orientation plan, in both Krapina and the EH sample, the CTC is on average, thicker anteriorly (aCTT > pCTT; Table 1), but intra-individual deviation from this pattern has been found in both assemblages (one case in Krapina and 23% and 14% of cases in the comparative sample for the sagittal and the transversal plane, respectively). In all cases and in both samples, CTT variation is size-independent (Table S3).

The specimens Pa. 1 and Pa. 5, suggested to represent the same individual (Trinkaus, 1975, 2000), are close for the sagittal anterior and transversal posterior average CTTs, but slightly distinguishable for the transversal aCTT (7.4% and 5.9%, respectively), the left patella Pa. 5 systematically displaying a slightly thinner shell (Table 1, Figure S1a,c, Table S2). Slightly higher differences in CTC arrangement are recorded between Pa. 3 and Pa. 14, the second possible individual pair of patellae within the Krapina's assemblage included in this study (Trinkaus, 2000). In this case, the greatest difference concerns the transversal pCTT (5.6% and 3.1%, respectively; Table 1, Figure S1b,f, Table S2). However, compared with the homologous
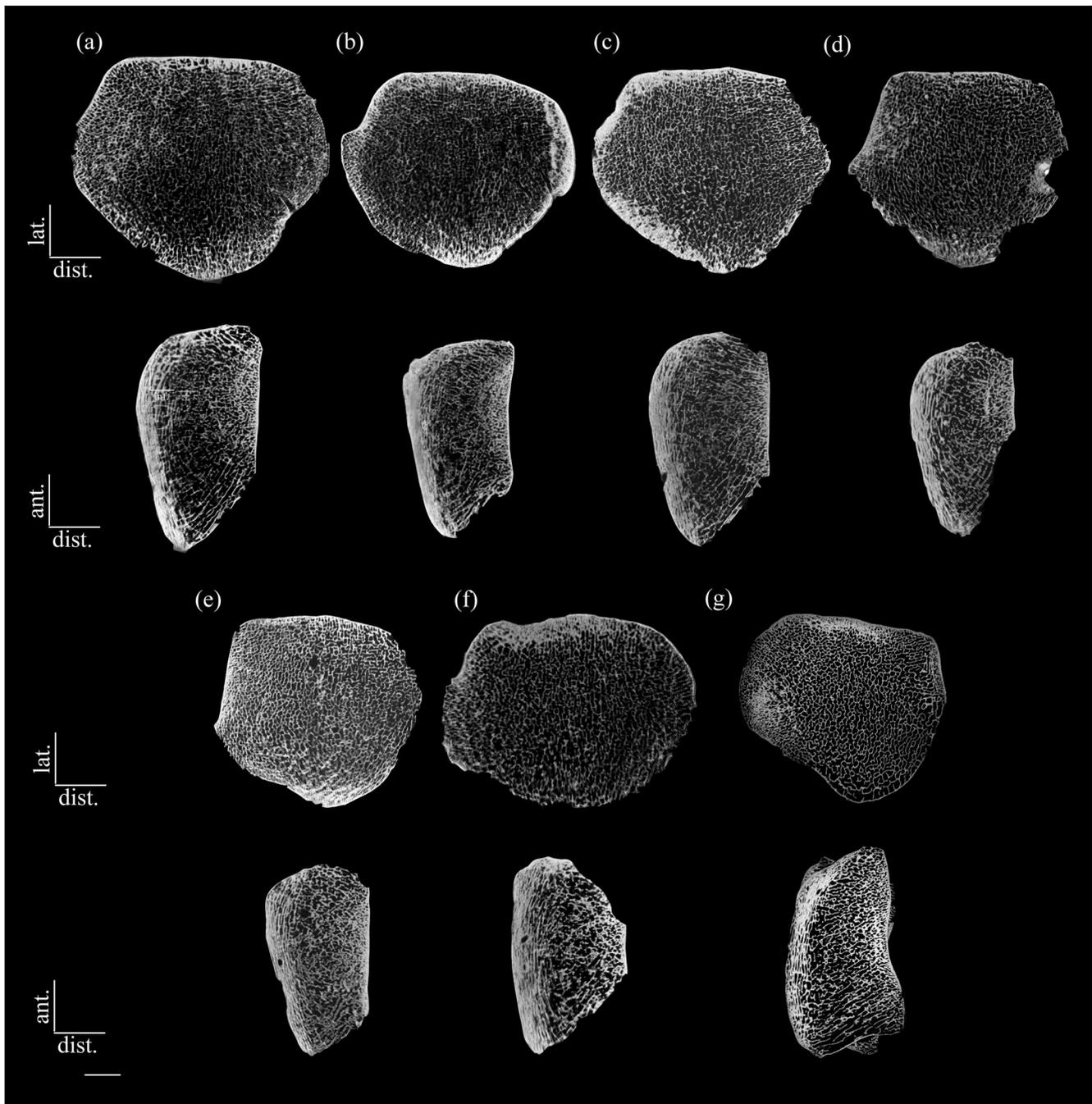
FIGURE 3 Coronal (upper row) and sagittal (lower) virtual sections extracted across the center of the right patella 215.1-Pa. 1 (a), the right patella 215.3-Pa. 3 (b), the left patella 216.1-Pa. 5 (c), the right patella 215.5-Pa. 6 (d), the left patella 216.3-Pa. 8 (e), the left patella 216.9-Pa. 14 (f) from Krapina, and of an extant human (EH) representative (g; a 22 years old female). Scale bar: 1 cm.

values of CTC cross-sectional differences measured for the eight pairs of patellae representing as many individuals from the Pretoria Bone Collection (Table S1), where fluctuating (nondirectional) asymmetry ranges between 0.1% and 3.2%, with no pattern of laterality (Table S4), the differences recorded within the possible pairs Pa. 1-Pa. 5 and Pa. 3-Pa. 14 (range < 2.5%) are fully compatible with intra-individual normal variation. We, therefore, cannot reject the hypothesis that Pa. 1-Pa. 5 are from the same individual as well as Pa. 3-Pa. 14 (Trinkaus, 1975, 2000).

3.2 | Trabecular bone structural organization

The individual and average values of the structural properties of the trabecular network assessed in the patellae from Krapina and the average values measured in the comparative EH sample for the proximal (s), distal (i), medial (m), and lateral (l) VOIs are shown in Table 2 and rendered in Figure 4.

The Neanderthal values do not significantly differ from the EH estimates but for the degree of anisotropy (DA) of the dVOI and for

CAZENAVE and RADOVČIĆ

AMERICAN JOURNAL OF
BIOLOGICAL ANTHROPOLOGY
The Official Journal of the American Association of Biological Anthropologists

WILEY 7

TABLE 1 Individual and mean values of the mean cortico-trabecular thickness (CTT, standardized % values) measured for the anterior (aCTT) and posterior (pCTT) aspects across the sagittal and transversal virtual slices, respectively (Figure 2a), in the Neanderthal patellae from Krapina and in the extant human (EH) reference sample used for comparisons ($n = 22$).

Specimen/sample	aCTT sagittal	pCTT sagittal	aCTT transversal	pCTT transversal
Krapina				
215.1-Pa. 1	8.0	6.7	7.4	5.8
215.3-Pa. 3	7.9	7.2	7.4	5.6
216.1-Pa. 5	8.0	7.0	5.9	4.5
215.5-Pa. 6	8.4	-	6.8	-
216.3-Pa. 8	8.8	10.6	9.7	6.4
216.9-Pa. 14	9.2	-	6.6	3.1
Mean (SD)	8.4 (0.5)	7.9 (1.9)	7.3 (1.3)	5.1 (1.3)
EH (SD)	8.3 (2.3)	7.1 (2.4)	6.7 (2.1)	4.8 (1.7)

the trabecular bone volume fraction (BV/TV) of the mVOI (Figure 4, Table S5; *p* values of 0.02 and 0.005 for the DA of the dVOI and BV/TV of the mVOI, respectively), the latter reflecting a higher average bulk density in the medial region characterizing the Neanderthal assemblage. Besides the dVOI DA, the differences between Krapina and the comparative sample measured for the other parameters of the medial and lateral VOIs slightly exceed those expressed between the proximal and distal VOIs. However, as already noted for the thickness of the CTC (Table 1), topographic variation of the trabecular network structural properties shown by the comparative human sample is higher than expressed by the Krapina assemblage by itself (Figure 4).

In all Neanderthal specimens, a structural reinforcement of the trabecular network indicated by higher BV/TV and Tb.Th. values is found in the lateral VOI (Table 2), whose values statistically differ from those measured in the other three VOIs (Table S6; *p* value of 0.03). A relative lateral reinforcement is also variably developed in the EH patellae (including comparing to humans from Cazenave et al., 2019, 2020; Tables 2 and S6), where it is associated with a proximal reinforcement of the network, this latter feature systematically lacking in Krapina (see also Cazenave et al., 2019, 2020; Toumi et al., 2006; Tables 2 and S6). Conversely, the Krapina assemblage and the EH networks share a relatively denser trabecular area approximately positioned at the proximolateral margin; a higher number of radially oriented trabeculae around the medial peripheral area; a vertically oriented anterior bundle; and two obliquely oriented proximal and distal bundle-like structures running from the anterior to the posterior endosteal surfaces (see also Cazenave et al., 2019, 2020).

Among all 12 variables examined for each sample (three structural properties by four VOIs), a significant correlation with the patellar mediolateral breadth has been recorded only for the medial DA in the fossil sample and the proximal BV/TV in the comparative human sample (Table S3).

The possible Krapina's pair Pa. 1-Pa. 5 shows some closer affinities in trabecular organization compared to the signal from other specimens forming the Neanderthal assemblage, but the two patellae differ for the BV/TV of the distal VOI (22.5% vs. 30.1%), the Tb.Th. of the lateral VOI (0.36 vs. 0.28 mm), and the DA of the distal VOIs (0.50 vs. 0.34). Conversely, for the mVOI DA (0.57 and 0.67, respectively) they show the highest values of the entire fossil assemblage (average

of the remaining specimens = 0.44). Structural affinities also exist between the specimens forming the other possible pair, Pa. 3 and Pa. 14, but in this case they differ for the BV/TV (25.8% vs. 38.0%) and the DA (0.24 vs. 0.50) of the dVOI (Table 2). Indeed, while Pa. 3 displays at all sites BV/TV values distal to the average of the whole fossil assemblage, Pa. 14 is among the most endostructurally robust specimens. As recorded for the thickness values of the CTC, even greater differences than those revealed by the comparative analysis of the two possible Neanderthal pairs Pa. 1-Pa. 5 and Pa. 3-Pa. 14 have been measured in our ad hoc sample of eight pairs of EH patellae (Table S7). As recorded for the CTC arrangement, no pattern of laterality between the paired patellae has been found in the EH sample for the structural properties of the trabecular network (Table S7), that can be associated to fluctuating asymmetry (i.e., small, random deviations away from perfect bilateral symmetry).

4 | DISCUSSION

The quantitative endostructural analysis of six patellae from the Neanderthal site of Krapina, Croatia, has revealed a modest degree of variation in cortical bone topographic distribution and site-specific arrangement of the trabecular network, associated with a lower degree of intra-individual organizational heterogeneity than commonly observed in EHs (Cazenave et al., 2019, 2020; Hoechel et al., 2015; Toumi et al., 2006, 2012; this study). This, despite a certain degree of dimensional and morphological variation displayed by the Krapina fossils in a number of outer features (e.g., expression of the vastus lateralis notch, concavity of the lateral articular facet and of the proximodistal profile of the articular crest; Radovčić et al., 1988; Rosas et al., 2020; Trinkaus, 2000; see Table S8). However, given the extremely limited size of the investigated Krapina sample, such observation needs confirmation.

In the Krapina assemblage, for most measures of cortico-trabecular thickness distribution and structural properties of the trabecular bone, a comparable structural signature is expressed by the two pairs of specimens Pa. 1 and Pa. 5, on the one side, and, to a lesser extent, Pa. 3 and Pa. 14, on the other side, originally suggested to likely represent two individuals because of their outer features and proportions (Trinkaus, 1975, 2000). Even though bony endostructure

TABLE 2 Individual and mean values of the bone volume fraction (BV/TV, in %), the trabecular thickness (Tb.Th., in mm) and the degree of anisotropy (DA) of the volumes of interest (VOIs) sampling the proximal (pVOI), distal (dVOI), medial (mVOI), and lateral (lVOI) regions (Figure 2b) measured in the Neanderthal patellae from Krapina and in the extant human (EH) reference sample used for comparisons (n = 22).

Specimen/sample	pVOI BV/TV	Tb.Th.	DA	dVOI BV/TV	Tb.Th.	DA	mVOI BV/TV	Tb.Th.	DA	lVOI BV/TV	Tb.Th.	DA
Krapina												
215.1-Pa. 1	33.1	0.29	0.55	22.5	0.24	0.50	38.3	0.29	0.57	44.8	0.36	0.49
215.3-Pa. 3	34.4	0.28	0.51	25.8	0.27	0.24	30.7	0.29	0.52	42.4	0.35	0.40
216.1-Pa. 5	38.7	0.30	0.57	30.1	0.27	0.34	39.0	0.27	0.67	43.8	0.28	0.56
215.5-Pa. 6	31.5	0.27	0.59	33.9	0.24	0.39	34.0	0.26	0.35	49.4	0.35	0.43
216.3-Pa. 8	36.3	0.28	0.66	39.0	0.26	0.43	34.8	0.25	0.34	45.2	0.30	0.70
216.9-Pa. 14	34.9	0.26	0.52	38.0	0.30	0.50	39.6	0.27	0.54	45.9	0.33	0.47
Mean	34.8	0.28	0.57	31.6	0.26	**0.40**	**36.1**	0.27	0.50	45.3	0.33	0.51
(SD)	(2.5)	(0.01)	(0.05)	(6.6)	(0.02)	(0.10)	(3.5)	(0.02)	(0.13)	(2.4)	(0.03)	(0.11)
EH (SD)	40.1 (9.9)	0.31 (0.13)	0.52 (0.19)	**30.0** (12.4)	0.24 (0.06)	**0.57** (0.17)	**28.8** (6.8)	0.24 (0.06)	0.51 (0.16)	41.8 (10.4)	0.34 (0.15)	0.49 (0.15)

Note: Significant differences (*p* value < 0.05) are shown in bold (see Table S5 for statistical results).

might locally vary under the influence of non-systemic factors (Saers et al., 2016; Tsegai et al., 2018) and, mostly, that the degree of intra-individual inner variation between left and right patella has not been assessed yet on representative reference samples, based on our comparative observations (eight EH cases examined for laterality), this suggestion cannot be rejected. Indeed, our comparative sub-sample of extant individuals expresses side differences greater than those shown by the two likely pairs of Neanderthal patellae. Accordingly, it is reasonable to assume that the sample of patellar bones from Krapina examined here (Radovčić et al., 1988) represents four adult individuals. While quantitatively very limited, it nonetheless represents the largest assemblage of human fossil patellae assessed so far for their endostructural conformation (cf. Cazenave et al., 2019, 2020). If so, in Krapina, the differences observed between the left and right patellae, that do not show a consistent trend between the investigated parameters might only represent fluctuating asymmetry.

Compared to the EH condition, while not necessarily to that expressed by Upper Paleolithic Eurasians (Trinkaus & Ruff, 2012), the Neanderthal appendicular skeleton, including the lower limb elements, commonly shows thicker cortices (cortical hypertrophy) (e.g., Churchill, 1998; Garralda et al., 2014; Kubicka et al., 2018; Mazurier et al., 2010; Mussini et al., 2012; Puymerail et al., 2012, 2013; Ruff et al., 1993, 1994; Trinkaus et al., 1999; Trinkaus & Ruff, 1989, 2012; Volpato et al., 2012), a feature thought to represent "the consequence of overall activity, through both mechanical and systemic (growth hormone) effects on bone modeling and remodeling across the entire skeleton" (Churchill, 1998, p. 58; but see Kubicka et al., 2022). Indeed, medullary stenosis has been found also in the adult Krapina's femora (Churchill, 1998; Kricun et al., 1999). However, even though slightly thicker on average, the cortex of the Krapina fossil patellae is hardly distinguishable from that measured in our human comparative sample. Accordingly, our first expectation of a higher amount of cortical bone characterizing the Krapina assemblage is rejected. Rather, the present results confirm our very preliminary observations performed on Pa. 5. and on the Neanderthal patella C3 90 from the likely late OIS 5 partial skeleton Regourdou 1, France (Madelaine et al., 2008; Maureille et al., 2015), indicating the lack of differences with respect to the EH figures in both cases (Cazenave et al., 2019, 2020). If supported by additional evidence, these results would indicate that the patellar bone did not follow the trend of generalized gracilization of the human postcranial skeleton recorded through the Upper Pleistocene (Ruff et al., 1994, 2015). In addition to a lack of significant differences in cortical bone volume of the patella between Krapina and EHs, our new observations show that, on average, the fossil and the human samples also share the same pattern of cortico-trabecular bone thickness distribution, that is, anterior sagittal > posterior sagittal > anterior transversal > posterior transversal.

Based on the outer characteristics distinguishing the Neanderthal from the modern human patella (Rosas et al., 2020; Trinkaus, 2000), we also expected the Krapina assemblage showing a number of distinctive features in site-specific trabecular network organization allowing to potentially define a "typical" Neanderthal endostructural
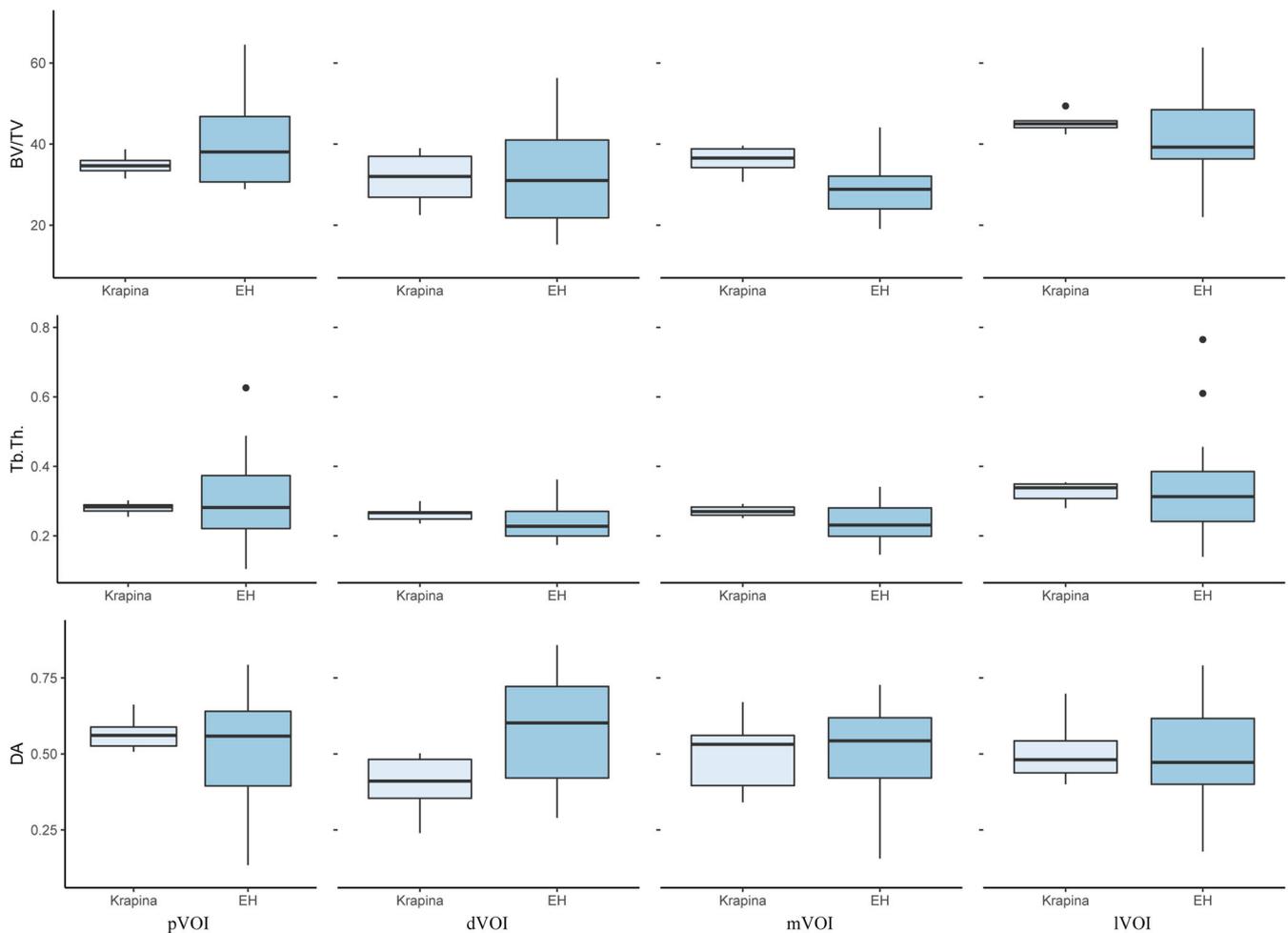
FIGURE 4 Boxplots of the median, SD, minimum and maximum values of the bone volume fraction (BV/TV, in %), trabecular thickness (Tb. Th., in mm) and degree of anisotropy (DA) of the proximal (pVOI), distal (dVOI), medial (mVOI), and lateral (lVOI) volumes of interest (VOIs) assessed in the Neanderthal sample of patellas from Krapina ($n = 6$) and the extant human (EH) reference sample used for comparisons ($n = 22$).

pattern. Differently from the first one, this second prediction is at least partially supported. Indeed, for their structural properties, the Krapina's patellae tend to differ from the recent human ones by showing a higher medial density (higher BV/TV and Tb.Th.) and by the lack of a proximal cancellous reinforcement, which is instead variably developed in the extant specimens. As a whole, this results into two generically distinct patterns for both the trabecular bone volume fraction and the trabecular thickness (but not for the degree of anisotropy): lateral > proximal ≅ distal ≅ medial, in Krapina, versus proximal ≅ lateral > distal ≅ medial, more typical in EHs.

Such reinforcements are interpreted as related to the mechanical stresses acting at the quadriceps tendon, but also to reflect a functional similarity in the action exerted by the central (vastus intermedius) and lateral (vastus lateralis) components of the quadriceps muscles (Toumi et al., 2012). Differently, the medial side of the patella, whose cancellous network is absolutely and relatively denser in the Krapina fossils, undergoes the loads of the medial component of the quadriceps (vastus medialis), which inserts obliquely on the patella to actively resist its lateral pull and contributes the medial stability of the

knee-joint (Balcarek et al., 2014; Rajput et al., 2017; Toumi et al., 2012). Accordingly, the endostructural configuration of the Krapina's patellae suggests a mechanical environment of the Neanderthal knee joint comparable to the EH condition for the loads exerted by the vastus lateralis, but not for those of the vastus medialis, whose functional action in the stabilization of the articulation might have been absolutely and relatively stronger than commonly occurs in EHs.

Besides some differences between Neanderthals and EHs in the relative development, positioning and function of the vastus muscles (e.g., Belcastro et al., 2006; Belcastro & Mariotti, 2017; Rosas et al., 2020), the influence on the Neanderthal knee joint of the greater robusticity of the distal femoral epiphysis remains also to be clarified. With this regard, a comparative study combining linear measurements and a 3D geometric morphometric analysis of the outer patella in a whole sample of 27 late Middle-Late Pleistocene Neanderthals (including four specimens from Krapina) has shown that Neanderthals had a more oblique attachment of the complete quadriceps muscular package expressed by a large size of the medial articular facet and a relative displacements of the medial and lateral masses

10 | WILEY—AMERICAN JOURNAL OF BIOLOGICAL ANTHROPOLOGY
The Official Journal of the American Association of Biological Anthropologists

CAZENAVE and RADOVČIĆ

of the patellar body than expressed in EHs. This configuration, compatible with the differences in the endostructural conformation of the trabecular network recorded in our study, has been related to a distinct rotation of the tibia with respect to the femur uniquely characterizing the Neanderthal knee joint, but interpreted as more likely representing a consequence of body form evolution in *Homo* rather than a specific functional adaptation of the knee (Rosas et al., 2020).

It is noteworthy that inter-individual variation in patellar endostructural arrangement expressed by our comparative extant sample is wide and a Krapina-like trabecular conformation pattern is also found in a couple of extant specimens used in this study. On the other hand, a previous analysis of the Regourdou 1's patella (Madelaine et al., 2008; Trinkaus, 2000; Vandermeersch, 1981), hardly distinguishable for its outer proportions and morphology from the average condition expressed by the Krapina assemblage (Table S8) and, more widely, by the Neanderthal condition (Rosas et al., 2020), has revealed a rather modern human-like cancellous pattern, with a lateral and proximal bone reinforcement (Cazenave et al., 2019, 2020). This suggests a potentially wide range of inter-population variation among Neanderthals. However, in the absence of comparative information from additional assemblages, the extent of such variation and any possible evidence for time- and geographic-related trends remain unknown.

Embedded within tendons and ligaments and acting "to protect the knee joint, to lengthen the lever arm of the quadriceps femoris, and to increase the area of contact between the patellar ligament and the femur" (White et al., 2012, p. 252), the patella adapts its outer and inner structure in response to the mechanical environment and the evolutionary changes in force transmission at the knee joint (Cazenave et al., 2019, 2020; Rosas et al., 2020; Toumi et al., 2006, 2012). In this view, the assessment of the evolutionary patterns of its endostructural conformation should provide subtle information of relevant biomechanical significance. However, the number of hominin fossil specimens examined so far is less than negligible and quantitative information on EH variation is also limited. Accordingly, future anthropological research should pay greater attention to comparatively detail the inner structural evolutionary anatomy of this bone in the hominin fossil record and to develop analyses on representative EH samples from various chrono-geographic contexts aimed at elucidating the influence of variables such as age, sex, body size and shape, physical activity, among others, on the variation patterns of its cortical bone topography and trabecular arrangement.

AUTHOR CONTRIBUTIONS

Marine Cazenave: Conceptualization (lead); formal analysis (lead); investigation (lead); methodology (lead). **Davorka Radovčić:** Data curation (lead); resources (supporting); validation (supporting); writing – review and editing (supporting).

ACKNOWLEDGMENTS

CONFLICT OF INTEREST STATEMENT

The authors declare no conflict of interest.

DATA AVAILABILITY STATEMENT

The data that support the findings of this study are available from the corresponding author upon reasonable request and upon permission of the Croatian Natural History Museum for the scans of the Neanderthal sample from Krapina.

ORCID

Marine Cazenave https://orcid.org/0000-0001-7194-5958

REFERENCES

Balcarek, P., Oberthür, S., Frosch, S., Schüttrumpf, J. P., & Stürmer, K. M. (2014). Vastus medialis obliquus muscle morphology in primary and recurrent lateral patellar instability. *BioMed Research International*, *2014*, 326586.

Beauchesne, P., & Agarwal, S. C. (2017). A multi-method assessment of bone maintenance and loss in an Imperial Roman population: Implications for future studies of age-related bone loss in the past. *American Journal of Physical Anthropology*, *164*, 41–61.

Belcastro, M. G. B., & Mariotti, V. (2017). A muscular imprint on the anterolateral surface of the proximal femurs of the Krapina Neandertal collection. *American Journal of Physical Anthropology*, *162*, 583–588.

Belcastro, M. G. B., Mariotti, V., Facchini, F., & Bonfiglioli, B. (2006). Musculoskeletal stress and adult age markers in the Krapina hominid collection: The study of femora 213 Fe. 1 and 214 Fe. 2. *Periodicum Biologorum*, *108*, 319–329.

Boule, M. (1911–1913). L'Homme fossile de la Chapelle aux-Saints. *Annales de Paléontologie*, *6*, 111–172 7, 21–56, 85–192; *8*, 1–70.

Cazenave, M. (2022). Functional insights from an exploration of the inner structure of the patella: new perspectives for the study of the hominin fossil record. Bulletins et mémoires de la Société d'Anthropologie de Paris. *BMSAP*, 34.

Cazenave, M., Oettlé, A., Thackeray, J. F., Nakatsukasa, M., de Beer, F., Hoffman, J., & Macchiarelli, R. (2019). The SKX 1084 hominin patella from Swartkrans Member 2, South Africa: An integrated analysis of its

outer morphology and inner structure. *Comptes Rendus Palevol*, 18, 223–235.

Cazenave, M., Radovčić, D., Hoffman, J., & Macchiarelli, R. (2020). The Neandertal (Krapina and Regourdou 1), fossil modern human (Chancelade 1) an extant human patella: An insight from inside. *Paleo*, 30, 76–91.

Chapman, T., Moiseev, F., Sholukha, V., Louryan, S., Rooze, M., Semal, P., & Jan, S. V. S. (2010). Virtual reconstruction of the Neandertal lower limbs with an estimation of hamstring muscle moment arms. *Comptes Rendus Palevol*, 9, 445–454.

Chirchir, H., Kivell, T. L., Ruff, C. B., Hublin, J. J., Carlson, K. J., Zipfel, B., & Richmond, B. G. (2015). Recent origin of low trabecular bone density in modern humans. *Proceedings of the National Academy of Sciences of the United States of America*, 112, 366–371.

Chirchir, H., Ruff, C. B., Junno, J. A., & Potts, R. (2017). Low trabecular bone density in recent sedentary modern humans. *American Journal of Physical Anthropology*, 162, 550–560.

Churchill, S. E. (1998). Cold adaptation, heterochrony, and Neandertals. *Evolutionary Anthropology*, 7, 46–60.

Dean, M. C., & Wood, B. A. (2003). A digital radiographic atlas of great apes skull and dentition. In L. Bondioli & R. Macchiarelli (Eds.), *Digital archives of human paleobiology 3*. ADS Solutions (CD-ROM).

Fajardo, R. J., Ryan, T. M., & Kappelman, J. (2002). Assessing the accuracy of high-resolution X-ray computed tomography of primate trabecular bone by comparisons with histological sections. *American Journal of Physical Anthropology*, 118, 1–10.

Fraipont, J. (1888). Le tibia dans la race de Néanderthal. *Revue d'Anthropologie*, 3, 145–158.

Garralda, M. D., Maureille, B., & Vandermeersch, B. (2014). Neanderthal infant and adult infracranial remains from Marillac (Charente, France). *American Journal of Physical Anthropology*, 155, 99–113.

Gorjanović-Kramberger, D. (1906). Der diluviale Mensch von Krapina in Kroatien. Ein Beitrag zur Paläoanthropologie. In O. Walkhoff (Ed.), *Studien über die Entwicklungsmechanik des primatenskeletes* (Vol. II, pp. 59–277). Kreidel.

Hartigan, E., Lewek, M., & Snyder-Mackler, L. (2011). The knee. In P. K. Levangie & C. C. Norkin (Eds.), *Joint structure and function* (5th ed., pp. 395–439). F. A. Davis.

Heim, J. L. (1982). Les hommes fossiles de La Ferrassie II. Les squelettes d'adultes (squelette des membres). *Archives de l'Institut de Paléontologie Humaine*, 38, 347–248.

Hoechel, S., Schulz, G., & Müller-Gerbl, M. (2015). Insight into the 3D-trabecular architecture of the human patella. *Annals of Anatomy-Anatomischer Anzeiger*, 200, 98–104.

Jungers, W. L. (1990). Scaling of postcranial joint size in hominoid primates. In F. K. Jouffroy, M. H. Stack, & C. C. Niemitz (Eds.), *Gravity, posture and locomotion in primates* (pp. 87–95). Editrice "Il Sedicesimo".

Katoh, T., Griffin, M. P., Wevers, H. W., & Rudan, J. (1996). Bone hardness testing in the trabecular bone of the human patella. *The Journal of Arthroplasty*, 11, 460–468.

Kricun, M., Monge, J., Mann, A., Finkel, G., Lampl, M., & Radovčić, J. (1999). *The Krapina hominids. A radiographic atlas of the skeletal collection*. Croatian Natural History Museum.

Kubicka, A. M., Nowaczewska, W., Balzeau, A., & Piontek, J. (2018). Bilateral asymmetry of the humerus in Neandertals, Australian aborigines and medieval humans. *American Journal of Physical Anthropology*, 167, 46–60.

Kubicka, A. M., Balzeau, A., Kosicki, J., Nowaczewska, W., Haduch, E., Spinek, A., & Piontek, J. (2022). Variation in cross-sectional indicator of femoral robusticity in Homo sapiens and Neandertals. *Scientific Reports*, 12, 4739.

L'Abbé, E. N., Loots, M., & Meiring, J. H. (2005). The Pretoria Bone Collection: A modern South African skeletal sample. *Homo*, 56, 197–205.

Lustig, W. (1915). Die Retroversion und Retroflexion der Tibia bei den Europäer-Neugeborenen in ihren Beziehungen zu den prähistorischen Menschenrassen. *Jenaische Zeitschrift Für Naturwissenschaft*, 53, 581–596.

Madelaine, S., Maureille, B., Cavanhie, N., Couture-Veschambre, C., Bonifay, E., Armand, D., Bonifay, M.-F., Duday, H., Fosse, P., & Vandermeersch, B. (2008). Nouveaux restes humains moustériens rapportés au squelette néandertalien de Regourdou 1 (Regourdou, commune de Montignac, Dordogne, France). *Paleo*, 20, 101–114.

Maureille, B., Gómez-Olivencia, A., Couture-Veschambre, C., Madelaine, S., & Holliday, T. (2015). Nouveaux restes humains provenant du gisement de Regourdou (Montignac-sur-Vézere, Dordogne, France). *Paleo*, 26, 117–138.

Mazurier, A. (2006). *Relations entre comportement locomoteur et variation cortico-trabéculaire du plateau tibial chez les primates: analyse quantitative non invasive à haute résolution (SR-·μCT) et applications au registre fossile* [Doctoral dissertation] Poitiers.

Mazurier, A., Nakatsukasa, M., & Macchiarelli, R. (2010). The inner structural variation of the primate tibial plateau characterized by high-resolution microtomography. Implications for the reconstruction of fossil locomotor behaviours. *Comptes Rendus Palevol*, 9, 349–359.

Miller, J. A., & Gross, M. M. (1998). Locomotor advantages of Neandertal skeletal morphology at the knee and ankle. *Journal of Biomechanics*, 31, 355–361.

Mussini, C., Crevecoeur, I., Garralda, M. D., Mann, A., & Maureille, B. (2012). A new neandertal femoral diaphysis from Les Pradelles (Marillac-le-Franc, Charente, France). *Periodicum Biologorum*, 114(1), 117–123.

Pina, M., Almécija, S., Alba, D. M., O'Neill, M. C., & Moyà-Solà, S. (2014). The Middle Miocene ape Pierolapithecus catalaunicus exhibits extant great ape-like morphometric affinities on its patella: Inferences on knee function and evolution. *PLoS One*, 9(3), e91944.

Puymerail, L., Volpato, V., Debénath, A., Mazurier, A., Tournepiche, J. F., & Macchiarelli, R. (2012). A Neanderthal partial femoral diaphysis from the "grotte de la Tour", La Chaise-de-Vouthon (Charente, France): Outer morphology and endostructural organization. *Comptes Rendus Palevol*, 11(8), 581–593.

Puymerail, L., Condemi, S., & Debénath, A. (2013). Comparative structural analysis of the Neanderthal femoral shafts BD 5 (MIS 5 e) and CDV-Tour 1 (MIS 3) from La Chaise-de-Vouthon, Charente, France. *PALEO. Revue D'archéologie Préhistorique*, 24, 257–270.

R Core Team. (2018). *R: A language and environment for statistical computing*. R Foundation for Statistical Computing http://www.R-project.org/

Radovčić, J., Smith, F. H., Trinkaus, E., & Wolpoff, M. H. (1988). *The Krapina hominids. An illustrated catalog of skeletal collection*. Croatian Natural History Museum.

Rajput, H. B., Rajani, S. J., & Vaniya, V. H. (2017). Variation in morphometry of vastus medialis muscle. *Journal of Clinical and Diagnostic Research*, 11, AC01-AC04.

Raux, P., Townsend, P. R., Miegel, R., Rose, R. M., & Radin, E. L. (1975). Trabecular architecture of the human patella. *Journal of Biomechanics*, 8, l-7.

Rink, W. J., Schwarcz, H. P., Smith, F. H., & Radovčić, J. (1995). ESR ages for Krapina hominids. *Nature*, 378, 24.

Rosas, A., Agustina, B. L., García-Martínez, D., Torres-Tamayo, N., García-Tabernero, A., Pastor, J. F., de la Rasilla, M., & Bastir, M. (2020). Analyses of the Neandertal patellae from El Sidrón (Asturias, Spain) with implications for the evolution of body form in *Homo*. *Journal of Human Evolution*, 141, 102738.

Ruff, C. B., Trinkaus, E., Walker, A., & Larsen, C. S. (1993). Postcranial robusticity in *Homo*, I: Temporal trends and mechanical interpretations. *American Journal of Physical Anthropology*, 91, 21–53.

Ruff, C. B., Walker, A., & Trinkaus, E. (1994). Postcranial robusticity in Homo. III: Ontogeny. *American Journal of Physical Anthropology*, 93, 35–54.

Ruff, C. B., Holt, B., Niskanen, M., Sladek, V., Berner, M., Garofalo, E., Garvin, H. M., Hora, M., Junno, J.-A., Schuplerova, E., Vilkama, R., &

Whittey, E. (2015). Gradual decline in mobility with the adoption of food production in Europe. *Proceedings of the National Academy of Sciences of the United States of America*, 112(23), 7147–7152.

Ryan, T. M., & Shaw, C. N. (2015). Gracility of the modern *Homo sapiens* skeleton is the result of decreased biomechanical loading. *Proceedings of the National Academy of Sciences of the United States of America*, 112(2), 372–377.

Ryan, T. M., & Ketcham, R. (2002). The three-dimensional structure of trabecular bone in the femoral head of strepsirrhine primates. *Journal of Human Evolution*, 43, 1–26.

Saers, J. P., Cazorla-Bak, Y., Shaw, C. N., Stock, J. T., & Ryan, T. M. (2016). Trabecular bone structural variation throughout the human lower limb. *Journal of Human Evolution*, 97, 97–108.

Scherf, H., Wahl, J., Hublin, J. J., & Harvati, K. (2016). Patterns of activity adaptation in humeral trabecular bone in Neolithic humans and present-day people. *American Journal of Physical Anthropology*, 159(1), 106–115.

Spoor, F., Zonneveld, F., & Macho, G. (1993). Linear measurements of cortical bone and dental enamel by computed tomography: Applications and problems. *American Journal of Physical Anthropology*, 91, 469–484.

Tardieu, C., & Trinkaus, E. (1994). The early ontogeny of the human femoral bicondylar angle. *American Journal of Physical Anthropology*, 95, 183–195.

Toumi, H., Higashiyama, I., Suzuki, D., Kumai, T., Bydder, G., Mcgonagle, D. D., Emery, P., Fairclough, J., & Benjamin, M. (2006). Regional variations in human patellar trabecular architecture and the structure of the proximal patellar tendon enthesis. *Journal of Anatomy*, 208, 47–57.

Toumi, H., Larguech, G., Filaire, E., Pinti, A., & Lespessailles, E. (2012). Regional variations in human patellar trabecular architecture and the structure of the quadriceps enthesis: A cadaveric study. *Journal of Anatomy*, 220, 632–637.

Townsend, P. R., Raux, P., Rose, R. M., Miegel, R. E., & Radin, E. L. (1975). The distribution and anisotropy of the stiffness of cancellous bone in the human patella. *Journal of Biomechanics*, 8, 363–367.

Trinkaus, E. (1975). The Neandertals from Krapina, northern Yugoslavia: An inventory of the lower limb remains. *Zeitschrift für Morphologie und Anthropologie*, 67, 44–59.

Trinkaus, E. (1983a). *The Shanidar Neandertals*. Academic Press.

Trinkaus, E. (1983b). Neandertal postcrania and the adaptive shift to modern humans. In E. Trinkaus (Ed.), *The Mousterian legacy: Human biocultural change in the Upper Pleistocene* (pp. 165–200). British Archaeological Reports.

Trinkaus, E. (2000). Human patellar articular proportions: Recent and Pleistocene patterns. *Journal of Anatomy*, 196, 473–483.

Trinkaus, E. (2006). The lower limb remains. In E. Trinkaus & J. Svoboda (Eds.), *Early modern human evolution in Central Europe: The people of Dolní Věstonice and Pavlov* (pp. 380–418). Oxford University Press.

Trinkaus, E., Churchill, S. E., Ruff, C. B., & Vandermeersch, B. (1999). Long bone shaft robusticity and body proportions of the Saint-Césaire 1 Châtelperronian Neanderthal. *Journal of Archaeological Science*, 26, 753–773.

Trinkaus, E., & Rhoads, M. L. (1999). Neandertal knees: Power lifters in the Pleistocene? *Journal of Human Evolution*, 37, 833–859.

Trinkaus, E., & Ruff, C. B. (1989). Diaphyseal cross-sectional morphology and biomechanics of the Fond-de-Forêt 1 femur and the Spy 2 femur and tibia. *Bulletin de la Société Royale Belge d'Anthropologie et de Préhistoire*, 100, 33–42.

Trinkaus, E., & Ruff, C. B. (2012). Femoral and tibial diaphyseal cross-sectional geometry in Pleistocene *Homo*. *PaleoAnthropology*, 2012, 13–62.

Trinkaus, E., Wojtal, P., Wilczyński, J., Sázelová, S., & Svoboda, J. (2017). Palmar, patellar and pedal human remains from Pavlov. *PaleoAnthropology*, 2017, 73–101.

Tsegai, Z. J., Skinner, M. M., Pahr, D. H., Hublin, J.-J., & Kivell, T. L. (2018). Systemic patterns of trabecular bone across the human and chimpanzee skeleton. *Journal of Anatomy*, 232, 641–656.

Tuniz, C., Bernardini, F., Cicuttin, A., Crespo, M. L., Dreossi, D., Gianoncelli, A., Mancini, L., Mendoza Cuevas, A., Sodini, N., Tromba, G., Zanini, F., & Zanolli, C. (2013). The ICTP-Elettra X-ray laboratory for cultural heritage and archaeology. *Nuclear Instruments and Methods in Physics Research Section A: Accelerators, Spectrometers, Detectors and Associated Equipment*, 711, 106–110.

Van Kampen, A., & Huiskes, R. (1990). The three-dimensional tracking pattern of the human patella. *Journal of Orthopaedic Research*, 8, 372–382.

Vandermeersch, B. (1981). *Les hommes fossiles de Qafzeh (Israël)*. CNRS.

Volpato, V., Macchiarelli, R., Guatelli-Steinberg, D., Fiore, I., Bondioli, L., & Frayer, D. W. (2012). Hand to mouth in a Neandertal: Right handedness in Regourdou 1. *PLoS One*, 7, 1–7 (e43949).

White, T. D., Black, M. T., & Folkens, P. A. (2012). *Human osteology* (3rd ed.). Academic Press.

Wickham, H. (2009). *ggplot2: Elegant graphics for data analysis*. Springer-Verlag.

SUPPORTING INFORMATION

Additional supporting information can be found online in the Supporting Information section at the end of this article.